

Quinolines and Oxazino-quinoline Derivatives as Small Molecule GLI1 Inhibitors Identified by Virtual Screening

Fabrizio Manetti,* Luisa Maresca, Enrica Crivaro, Sara Pepe, Elena Cini, Snigdha Singh, Paolo Governa, Samuele Maramai, Giuseppe Giannini, Barbara Stecca,* and Elena Petricci*



Cite This: *ACS Med. Chem. Lett.* 2022, 13, 1329–1336



Read Online

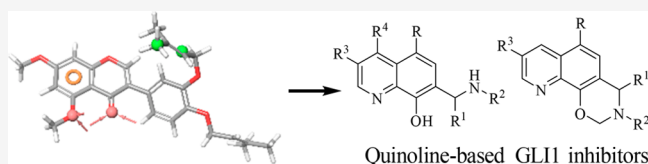
ACCESS |

Metrics & More

Article Recommendations

Supporting Information

ABSTRACT: A virtual screening approach based on a five-feature pharmacophoric model for negative modulators of GLI1 was applied to databases of commercially available compounds. The resulting quinoline derivatives showed significant ability to reduce the GLI1 protein level and were characterized by submicromolar antiproliferative activity toward human melanoma A375 and medulloblastoma DAOY cell lines. Decoration of the quinoline ring and chemical rigidification to an oxazino-quinoline scaffold



Quinoline-based GLI1 inhibitors

allowed us to deduce SAR considerations for future ligand optimization.

KEYWORDS: *GLI1 negative modulators, quinoline, Hedgehog pathway, anticancer agents, pharmacophoric model, virtual screening*

The canonical Hedgehog-GLI (Hh) pathway is initiated by binding of Hh ligands to the receptor Patched (PTCH1), which releases the inhibition of the transmembrane G protein coupled receptor Smoothed (SMO). The latter, in turn, triggers an intracellular cascade, which leads to the activation of the GLI transcription factors (TFs). There is also a noncanonical activation of the GLI TFs, which can be PTCH-SMO-independent and is triggered by several oncogenic signaling pathways.¹ The Hh signaling can be inhibited at the level of SMO or the TFs GLI1/2. SMO is the main target of Hh inhibition. So far, five inhibitors of SMO (namely, NVP-LDE225, referred to as Sonidegib or Erismodegib, and NVP-LEQ506, referred to as LEQ506, both by Novartis; PF-04449913, referred to as Glasdegib by Pfizer; BMS-833923, referred to as XL139 by Exelixis and out-licensed to Bristol-Myers Squibb; GDC-0449, referred to as Vismodegib by Genentec) accessed clinical trials and instilled hope for the treatment of human cancers such as medulloblastoma and basal cell carcinoma, which depend on the canonical Hh pathway activation. On the contrary, the same compounds were unsuccessful in treating many solid tumors that are dependent on the noncanonical activation of GLI1.¹ Indeed, negative modulators of GLI1 are currently represented by small molecules that can interfere with both canonical and noncanonical Hh signaling. Based on these results and considering that SMO inhibitors often select resistant mutations (primary or secondary resistance),^{2,3} many efforts were focused on the identification of small molecules able to directly target GLI1 and negatively modulate its activity.^{4–10} Few GLI1/2 inhibitors were identified thus far. The first GLI1/2 inhibitor described was GANT61, which blocks translocation of GLI1 to the nucleus and its binding to

DNA.^{11,12} Arsenic trioxide, which is not a specific GLI1 inhibitor, was shown to abrogate ciliary accumulation of GLI2¹³ and to reduce GLI1 mRNA and protein levels.¹⁴ Moreover, polyunsaturated fatty acids showed the ability to inhibit GLI.¹⁵ Additional small molecules identified by virtual screening approaches were also described in recent years. Unfortunately, toxicity and poor drug likeness are two major limitations of currently available GLI1 inhibitors.^{4,6,16}

Recently, glabrescione B (GlaB, Table 1)¹⁷ was used by us as the initial scaffold for the generation of a five-feature pharmacophoric model that led to the identification of negative modulators of GLI1 belonging to the classes of thiophene and pyrazolo-pyrimidine small molecules that populated databases of commercially available compounds.¹⁸ In addition, the same pharmacophore allowed the prioritization of several 8-hydroxyquinoline derivatives as putative GLI1 binders that are described here. Such compounds showed a scaffold similar to that of an 8-hydroxyquinoline derivative identified by a structure-based virtual screening protocol based on biased molecular docking simulations that was focused on the binding site of GANT61 within the structural region of GLI1 comprised between zinc-fingers 2 and 3.¹⁹

As a result of our pharmacophore-based virtual screening on databases of commercially available compounds, **1** was identified as a small molecule able to fully match the five

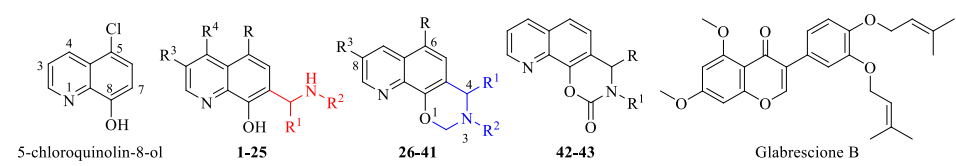
Received: May 26, 2022

Accepted: July 12, 2022

Published: July 22, 2022



Table 1. Chemical Structure, Antiproliferative Activity, and Effect on GLI1 Properties of the Quinoline and Oxazino-Quinoline Derivatives



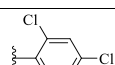
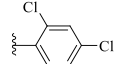
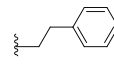
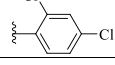
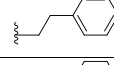
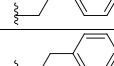

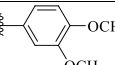
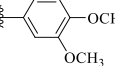
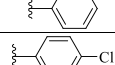
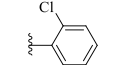
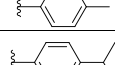
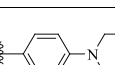
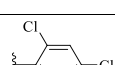
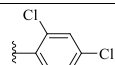
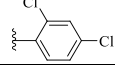
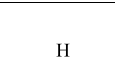
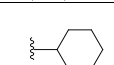
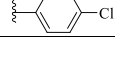
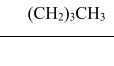



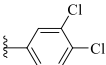
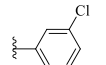
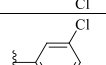
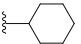
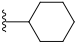
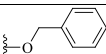
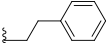
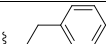
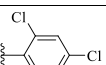
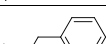
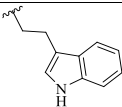
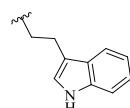
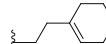
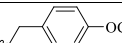
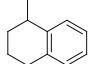


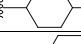
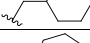
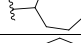
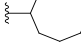
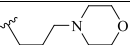
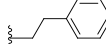
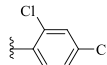
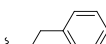
Compound ^a	R	R ¹	R ²	R ³	R ⁴	Antiproliferative activity ^b		Effect on GLI1 protein ^c
						Daoy	A375	
5-chloroquinolin-8-ol						ND	ND	NA
1 BAS02169272	Cl		CO(CH ₂) ₂ CH ₃	H	H	0.19 ± 0.01	0.11 ± 0.01	+++
2	H			H	H	0.15 ± 0.01	0.19 ± 0.02	+++
3	H			Me	H	ND	ND	NA
4	Cl	H		H	H	ND	ND	NA
5	H	H		H	H	0.33 ± 0.06	0.39 ± 0.1	+++
6 BAS01923177	Cl		COCH ₃	H	H	0.21 ± 0.01	0.11 ± 0.01	+++
7 BAS02169265	Cl		COCH(CH ₃) ₂	H	H	0.10 ± 0.008	0.13 ± 0.01	++
8 BAS01277891	H		CO(CH ₂) ₂ CH ₃	H	H	0.11 ± 0.01	0.13 ± 0.01	+++
9 BAS02169242	Cl		CO(CH ₂) ₂ CH ₃	H	H	0.11 ± 0.01	0.13 ± 0.01	NA
10 BAS02169266	Cl		CO(CH ₂) ₂ CH ₃	H	H	0.10 ± 0.01	0.12 ± 0.01	NA
11 BAS02169269	Cl		CO(CH ₂) ₂ CH ₃	H	H	0.10 ± 0.008	0.10 ± 0.007	+
12 BAS02169260	Cl		CO(CH ₂) ₂ CH ₃	H	H	0.10 ± 0.009	0.12 ± 0.009	+
13 BAS02169280 8B	Cl		CO(CH ₂) ₂ CH ₃	H	H	0.09 ± 0.01	0.12 ± 0.03	+++
14 BAS02169282	Cl		CO(CH ₂) ₂ CH ₃	H	H	0.10 ± 0.009	0.13 ± 0.02	+++
15	H			H	H	0.24 ± 0.04	1.01 ± 0.06	+++
16	H			H	H	0.15 ± 0.04	0.32 ± 0.04	+
17	H		(CH ₂) ₃ CH ₃	H	H	0.15 ± 0.05	1.12 ± 0.38	+++
18	H	H	(CH ₂) ₃ CH ₃	H	H	ND	ND	NA
19	H	H		H	H	0.72 ± 0.11	0.91 ± 0.18	+
20	H		(CH ₂) ₃ CH ₃	H	H	0.33 ± 0.11	0.71 ± 0.14	+++

Table 1. continued

Compound ^a	R	R ¹	R ²	R ³	R ⁴	Antiproliferative activity ^b		Effect on GLI1 protein ^c
						Daoy	A375	
21	H		(CH ₂) ₃ CH ₃	H	H	0.10 ± 0.02	0.32 ± 0.07	+
22	H		(CH ₂) ₃ CH ₃	H	H	0.14 ± 0.06	0.09 ± 0.01	++
23	H		(CH ₂) ₃ CH ₃	H	H	ND	ND	NA
24	H	H		H	O(CH ₂) ₃ CH ₃	0.51 ± 0.04	0.54 ± 0.06	+
25	H	H		H		0.26 ± 0.05	0.55 ± 0.07	+
26	H	H		H		0.19 ± 0.03	0.13 ± 0.05	++
27	H	H		F		1.4 ± 0.7	1.1 ± 0.3	++
28	H			H		ND	ND	NA
29	H	H		H		ND	ND	NA
30	Cl	H		H		ND	ND	NA
31 AKos807980	Cl	H		H		0.23 ± 0.08	0.12 ± 0.04	++
32	H	H		H		0.87 ± 0.12	0.58 ± 0.07	+
33	H	H		H		0.60 ± 0.2	0.30 ± 0.04	++
34	H	H		H		0.50 ± 0.03	0.30 ± 0.13	+++
35	H	H		F		0.3 ± 0.04	0.5 ± 0.06	+
36	H	H		H		0.55 ± 0.07	0.42 ± 0.03	++
37	H	H		H		1.0 ± 0.21	0.38 ± 0.04	+
38	H	H		H		1.2 ± 0.35	0.88 ± 0.02	+
39	H	H		H		0.29 ± 0.11	0.28 ± 0.07	++
40 AKos806649	Cl	H	(CH ₂) ₃ CH ₃	H		0.38 ± 0.05	0.49 ± 0.09	++
41 AKos807979	Cl	H		H		1.2 ± 0.1	0.15 ± 0.08	+
42	H					ND	ND	NA
43						ND	ND	NA
Glabrescione B ^d						0.13 ± 0.01	0.40 ± 0.2	+++

^aCompounds also labeled with BAS and AKos notations were purchased from Asinex and AKos vendors, respectively. ^bExpressed as IC₅₀ values (micromolar concentrations) calculated using GraphPad Prism V6 from triplicate experiments in melanoma (A375) and medulloblastoma (DAOY) cells. ND: not determined. ^cThe GLI1 protein level was determined by Western blotting (see Figure 4 for details) in murine NIH3T3 cells treated with SAG (100 nM), each compound (1 μM), and GANT61 (5 μM) for 48 h. NA: not affected; weakly reduced: +; reduced: ++; strongly reduced: +++. ^dActivity data taken from ref 18.

pharmacophoric features (Figure 1): the quinoline nitrogen and the oxygen atom of the phenol substituent represented the

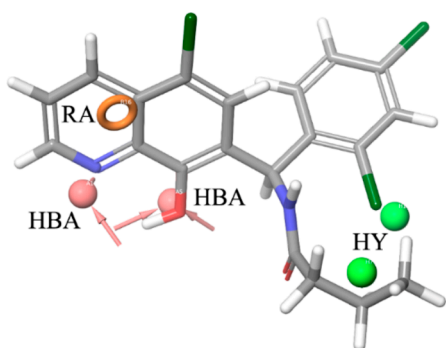


Figure 1. Graphical representation of **1** superposed to the five-feature pharmacophoric model for GLL1 negative modulators. The hydrogen bond acceptor (HBA) groups are represented by the quinoline nitrogen atom and the oxygen atom at C8 of the quinoline ring. The terminal propyl substituent and the 2-Cl at the pendant phenyl ring fit the hydrophobic regions (HYs). Finally, the pyridine ring corresponds to the ring aromatic (RA) feature.

hydrogen bond acceptors (HBAs), while the terminal propyl chain together with the 2-Cl substituent at the pendant phenyl ring were superposed to the hydrophobic features (HYs). Finally, the ring aromatic (RA) feature was fitted by the pyridine ring. Such a compound strongly reduced the GLL1 protein level in murine NIH3T3 cells treated with 100 nM SAG and 1 μ M test compound for 48 h. Moreover, a submicromolar antiproliferative activity was found toward the medulloblastoma DAOY and the melanoma A375 cell lines (IC_{50} = 0.19 and 0.11 μ M, respectively, Table 1). Overall activity found for **1** was comparable to that of GlaB (IC_{50} = 0.13 and 0.40 μ M, respectively, and a strong reduction of GLL1 level, Table 1).

A computational protocol previously described by us^{20–22} was used to identify putative binding sites on GLL1 and to prioritize new ligands for these pockets. In details, the SiteMap

routine of the Glide software was applied to the crystallographic five-finger structure of GLL1²³ with the aim of finding putative binding sites for small molecule ligands. Molecular docking simulations of **1** were then focused into the two putative binding sites identified by SiteMap. As a result, a best scored binding pose was characterized by an extended network of hydrogen bonds (Figure 2, left, and Figure 3). In particular,

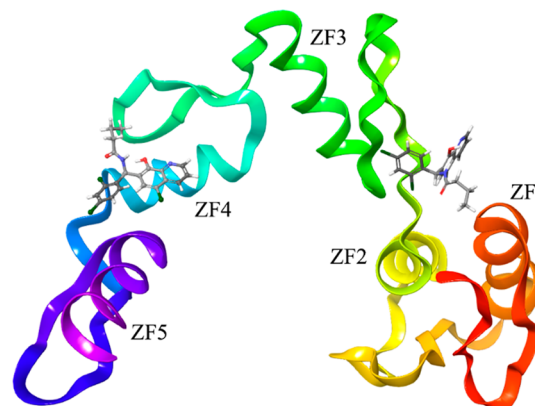


Figure 3. Graphical representation of the zinc-finger portion of the GLL1 structure, as stored in the entry 2gli of the Protein Data Bank.²³ Two alternative best-docked binding poses of the pyridine derivatives are also represented to show the locations of the different binding sites identified by the SiteMap routine of the Schrodinger suite. One binding site is located within the zinc-finger 4, while an alternative binding region is between the zinc-fingers 1 and 3, and it was hypothesized as the binding region of GANT61¹² and another 8-hydroxyquinoline derivative.¹⁹

the pyridine ring made a π -cation interaction with Arg223 of the zinc-finger 4 (numbers of amino acids refer to the 2gli structure reported in the Protein Data Bank; the corresponding UNIPROT numbers can be obtained by adding 131 units: as an example, the Arg223 reported in the Protein Data Bank corresponds to Arg354 of the UNIPROT P08151 sequence), and the quinoline nitrogen atom gave a hydrogen bond with

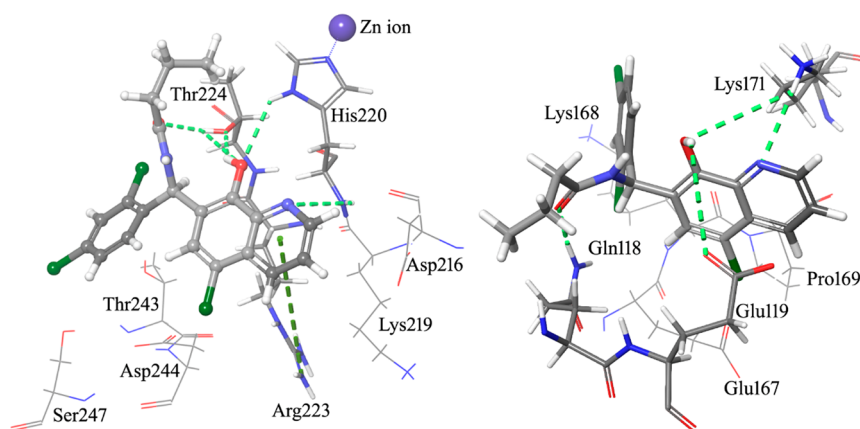


Figure 2. Graphical representation of the best-docked binding poses of **1** (ball & stick and element + gray carbon notations) within the structure of GLL1. A complex network of hydrogen bonds (light green dashed lines) is formed by GLL1 and the ligand. Left: The quinoline nitrogen, the 8-OH group, and the oxygen of the ester moiety form hydrogen bonds with the backbone and the side chain NH of His220 as well as with the side chain OH of Thr224. Moreover, the pyridine ring and the guanidino group of Arg223 give a π -cation interaction (green dashed line). Right: In an alternative binding pose, the terminal ammonium group of Lys171 makes hydrogen bonds with both the quinoline nitrogen and the 8-OH group of **1**. The latter substituent gives an additional hydrogen bond with the terminal carboxyl group of Glu119. The amide oxygen of the ligand and the terminal NH_2 of Gln118 provide another hydrogen bond. The propyl chain and the pendant phenyl ring make hydrophobic interactions with the target.

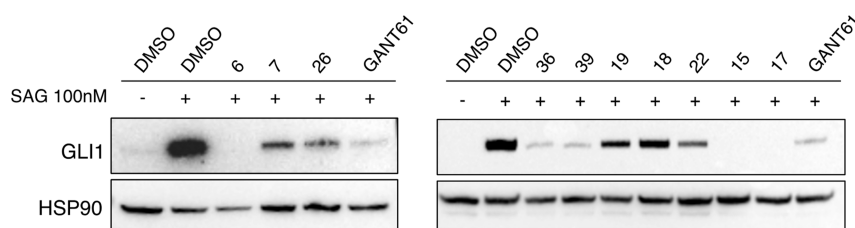


Figure 4. Representative Western blot of endogenous GLI1 in NIH3T3 cells stimulated with the Smoothed agonist SAG (100 nM) and treated with vehicle (DMSO), our putative GLI1 inhibitors (1 μ M), and GANT61 (5 μ M) for 48 h. HSP90 was used as loading control. See Table 1 for details.

the NH backbone moiety of His220 (one of the residues involved in coordination of a zinc ion). Moreover, the OH group of the ligand interacted with both the imidazole ring NH of His220 and with the hydroxyl group of Thr224, which in turn gave a hydrogen bond with the carbonyl oxygen of the ligand amide group. This binding pose, however, did not account for the hydrophobic features predicted by the pharmacophoric model. Among the best scored binding modes of **1**, an alternative pose was found (Figure 2, right, and Figure 3), where the ligand interacted with amino acids of the zinc-fingers 1 and 3, within the same binding pocket already found for another 8-hydroxyquinoline derivative¹⁹ and for the known GLI1 inhibitor GANT61.¹² The major anchor points were represented by hydrogen bonds between both the quinoline nitrogen and the 8-OH substituent with the terminal edge of Lys171, between the 8-OH group and the carboxyl moiety of Glu119, and between the amide oxygen of the ligand and the terminal NH₂ group of Gln118. Hydrophobic contacts were also found between the propyl terminal of **1** and the central portion of the Gln118 side chain as well as between the pendant phenyl ring and the central part of the Lys168 side chain.

Starting from the commercially available parent compound **1**, which was prioritized by the virtual screening approach, a focused library was built around the quinoline scaffold in the attempt to improve the biological profile and to deduce SAR considerations for further optimization. Table 1 summarizes the structure, antiproliferative activity, and ability to affect the GLI1 protein level of the new compounds. To assess the effects of compounds on GLI1 protein level, we used murine NIH3T3 cells, a well-established model to study the modulation of Hh signaling. Treatment of these cells with the SMO agonist SAG activates the endogenous Hh pathway. In Figure 4, we reported representative examples of compounds with different effects on the GLI1 protein level. For instance, **6**, **15**, and **17** strongly reduced GLI1 protein levels compared to SAG-treated NIH3T3 cells and were classified as “+++” (see Table 1). Compounds **7**, **26**, **36**, **39**, and **22** led to a moderate reduction of GLI1 protein expression and were classified as “++”. Compound **19** weakly reduced GLI1 protein expression and was classified as “+”. On the other hand, compound **18** did not affect GLI1 protein levels and was classified as “NA” (not affected).

Increasing the size and bulkiness of the propyl ester moiety into a phenylethylamino appendage and removing the chloride substituent at the C5 of **1** led to **2**, which retained a similar antiproliferative profile in DAOY and A375 cancer cells (IC₅₀ = 0.15 and 0.19 μ M) and a similar degree of reduction of GLI1. Insertion of a methyl group at the quinoline C3 as in **3** abrogated the activity on the GLI1 level. In a similar way, removal of the pendant phenyl ring as in **4** completely

abrogated reduction of GLI1 protein level that was fully restored by further removal of the C5 chlorine substituent as in **5**, together with a submicromolar antiproliferative activity (IC₅₀ = 0.33 and 0.39 μ M, respectively in DAOY and A375 cells).

Replacement of the dichloro substituents with a 3,4-dimethoxy substitution, independently from the length of the ester chain (methyl, isopropyl, and butyl as in **6**, **7**, and **8**, respectively) and the presence of a C5 chlorine substitution (R group) led to an antiproliferative activity in the submicromolar range (between 0.10 and 0.21 μ M) and a significant reduction of the GLI1 protein level. Worth noting, **6** strongly inhibited GLI1 expression (Figure 4). Further changing either the substituents or the substitution pattern on the pendant phenyl ring (at R¹) resulted in propyl or butyl esters that maintained the submicromolar antiproliferative activity, while the effect on GLI1 protein level was variable. As examples, the unsubstituted derivative **9** and the corresponding 4-Cl analogue **10** did not affect the GLI1 protein level, while the 2-Cl **11** and 4-Me **12** analogues showed weak reduction. A submicromolar antiproliferative activity and a strong reduction of the GLI1 protein level were also found for both the 4-*i*Pr and 4-diethylamino derivatives **13** and **14**, respectively.

Moreover, replacement of the ester or aryl side chain at R² with an alkyl or cycloalkyl substituent gave interesting results. As an example, **15** and its cyclopentyl and butyl analogues (**16** and **17**, respectively) significantly affected the GLI1 protein level (Figure 4) and showed micromolar antiproliferative activity, while the butyl analogue **18**, which was deprived of the pendant phenyl ring, was inactive. This result seemed to suggest the benzyl moiety at the quinoline C7 as an important substituent for activity, although the simplified analogue of **15** (namely, **19**) maintained micromolar antiproliferative activity and weak GLI1 protein level reduction. Moreover, the phenylethylamino derivative **4** was also inactive, while a good biological profile was restored when its C5 chlorine substituent was removed as in **5**.

Among butylamino analogues, compounds where the 2,4-diCl substituents and substitution pattern at R¹ were changed (as in **20**, **21**, and **22**), were characterized by a submicromolar antiproliferative activity and variable reduction of the GLI1 protein level. The sole exception was represented by the 3-Cl analogue **23** that was inactive.

Worth noting, insertion of an alkoxy substituent at the quinoline C4 of the cyclohexylamino derivative **19** (R⁴) led to **24** and **25**, which showed a slightly better antiproliferative activity (IC₅₀ between 0.26 and 0.55 μ M), with only a modest reduction of the GLI1 protein level.

Biological data on 8-hydroxyquinoline derivatives suggested several SAR considerations. The antiproliferative activity seemed to be slightly dependent on the substituents and

substitution pattern on the phenyl ring of the C7 benzyl moiety. In fact, IC_{50} values were in the single-digit micromolar or submicromolar range. On the contrary, the effect on the GLI1 protein level was affected by these molecular features. As an example, unsubstituted compounds (as **9**) or those bearing a small substituent (such as a Cl or Me as found in **10**, **11**, **23**, and **12**) showed low or no ability to affect the GLI1 protein level. An exception was represented by **20** that almost abrogated GLI1 protein expression. However, the C7 benzyl moiety was not a mandatory structural feature for compound activity. In fact, although the butyl derivative **18** was inactive, increasing the size of the R^2 substituent to a cyclohexyl ring (as in **19**, **25**, and **24**) gradually restored activity. Finally, the simple 5-chloroquinolyl-8-ol was inactive.

Following a structural rigidification strategy, the methan-amino moiety and the hydroxyl substituents present at the quinoline C7 and C8, respectively, were connected to give a condensed dihydro-1,3-oxazine ring. The *N*-phenylethyl analogue **26** showed submicromolar antiproliferative activity toward both cell lines ($IC_{50} = 0.19$ and $0.13 \mu\text{M}$, respectively, Table 1) and a significant reduction of the GLI1 protein level (Figure 4). Docking simulations showed a binding pose where the heteroatoms of the condensed scaffold were involved in a network of hydrogen bonds (Figure 5). In particular, the

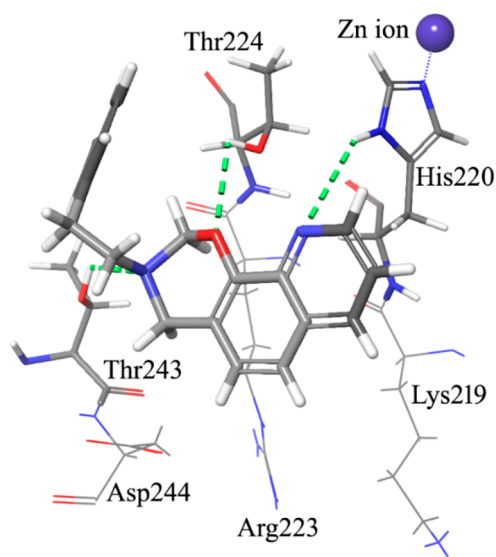


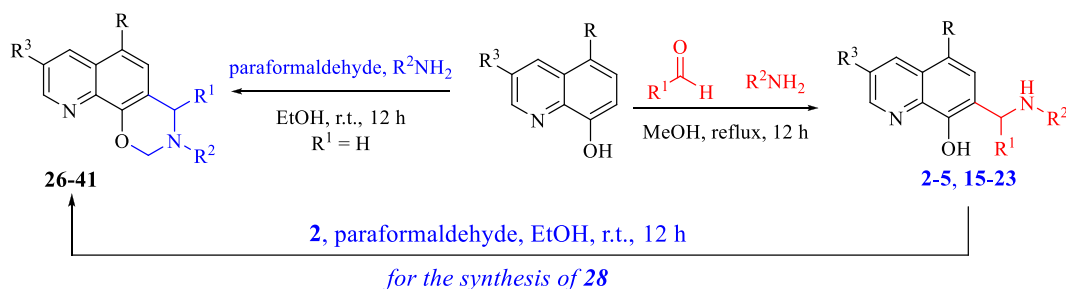
Figure 5. Graphical representation of the docked pose of the oxazino-quinoline derivative **26**. The quinoline nitrogen gives a hydrogen bond with the imidazole ring of His220. Two additional hydrogen bonds are made by the oxygen and the nitrogen atom of the oxazine ring with the side chain OH groups of Thr224 and Thr243.

nitrogen atom of the quinoline system interacted with the imidazole ring of His220, while the oxygen and nitrogen atoms of the oxazine ring gave hydrogen bonds with the hydroxyl groups of Thr224 and Thr243, respectively. Similarly to the 8-hydroxyquinoline derivatives, also the oxazino-quinoline showed an alternative best scored docking pose within the putative binding site of GANT61 (not shown).

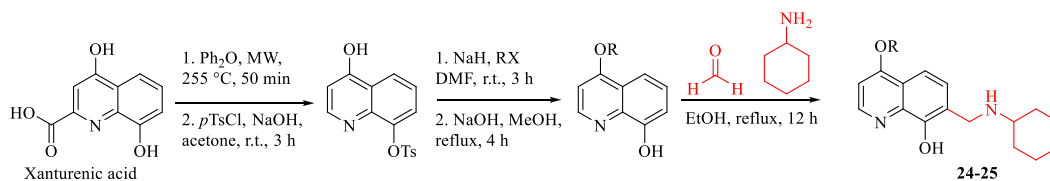
The antiproliferative activity decreased by about 10-fold in the C8 (the R^3 substituent) fluoro derivative **27** (IC_{50} between 1.4 and $1.1 \mu\text{M}$, respectively), and the insertion of a substituted phenyl ring at the oxazine C4 was further detrimental for the activity of **28** that was inactive. Replacing the pendant phenyl ring of **26** with an indolyl moiety resulted in **29** and **30** that were both inactive too. On the other hand, partial reduction of the phenyl moiety to a cyclohexene ring, shortening to a benzyl chain, and rigidification to a tetrahydronaphthyl ring led to **31**, **32**, and **33**, respectively, which showed submicromolar antiproliferative activity toward both cell lines (IC_{50} between 0.12 and $0.87 \mu\text{M}$) and a significant reduction of the GLI1 protein level. Interestingly, when the condensed phenyl ring of **33** was simplified to have the corresponding cyclohexyl analogue **34**, the antiproliferative activity was maintained, while the GLI1 protein level was strongly reduced. Insertion of a fluorine substituent at the quinoline C8 resulted in **35** with a reduced ability to affect the GLI1 protein level. Methylation at the cyclohexyl C4 of **34** resulted in **36** with a reduced activity. In a similar way, lengthening the R^2 side chain by insertion of a methylene bridge as in **37** maintained a micromolar antiproliferative activity but weakly affected the GLI1 protein level. Moreover, homologation of the cyclohexyl moiety of **34** into a cycloheptyl ring as in **38** caused a reduction of the antiproliferative activity and ability to affect the GLI1 protein level. An improvement of the biological profile was obtained with further enlargement to the octyl ring of **39** that showed $IC_{50} = 0.29$ and $0.28 \mu\text{M}$, respectively, and a significant reduction of GLI1 protein level. Simplification of the R^2 substituent to a butyl chain (as in **40**) retained interesting activity, while adding a morpholinyl appendage as in **41** negatively affected both the antiproliferative activity toward DAOY cells and the ability to reduce GLI1 protein level.

Among oxazino-quinoline condensed compounds, as a general rule, the presence of a C8 substituent was detrimental for activity (compare **34** with **35** and **26** with **27**), as well as the presence of a substituent at the C4 of the oxazine ring (compare **26** with **28**). On the other hand, the presence of a substituent at the C6 (the R substituent) did not affect the activity (compare **29** to **30**).

Scheme 1. Preparation of 2–5, 15–23, and 26–41



Scheme 2. Preparation of 4-OR Derivatives 24 and 25



Finally, transformation of the dihydro-1,3-oxazine ring into the corresponding *N*-phenylethyl cyclic carbamates yielded **42** and **43** that were inactive.

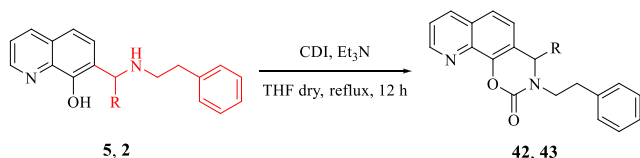
Overall, many of the quinoline derivatives showed an antiproliferative activity in the submicromolar range, significantly better (in general, at least 1 order of magnitude higher) in comparison to the thiophene and pyrazolo-pyrimidine compounds previously identified by means of the same pharmacophore model.¹⁸ Cyclization of the C7–C8 quinoline substituents to a condensed oxazine ring allowed a further enlargement of SAR considerations.

Expected derivatives **2–5** and **15–23** were efficiently synthesized starting from commercially available properly substituted 8-hydroxyquinolines by treatment with different aldehydes and amines in MeOH at reflux (Scheme 1). Tricyclic compounds **26–41** were obtained from the same starting materials by using paraformaldehyde and proper amines at room temperature in EtOH (Scheme 1).

For the preparation of 4-OR derivatives **24** and **25**, a decarboxylation of xanthurenic acid under microwave irradiation at 255 °C followed by a selective protection of the phenol moiety in the C-8 position were required (Scheme 2). The intermediates obtained were alkylated by treatment with the proper alkyl halide, deprotected, and functionalized at their C7 in the same reaction conditions reported for **2–5** and **15–23**.

Tricyclic carbamates **42** and **43** were prepared from **5** and **2**, respectively, by treatment with *N,N'*-carbonyldiimidazole (CDI) in the presence of Et₃N at reflux (Scheme 3).

Scheme 3. Preparation of Tricyclic Carbamates 42 and 43



In conclusion, a virtual screening procedure based on a five-feature pharmacophoric model led to prioritizing 8-hydroxyquinoline derivatives as negative modulators of GLI1 with submicromolar antiproliferative activity toward both human melanoma and medulloblastoma cell lines. Many of these compounds also showed ability to strongly reduce the GLI1 protein level in NIH3T3 cells. Decoration of the quinoline ring and its rigidification to an oxazino-quinoline moiety allowed to deduce SAR considerations that could be usefully applied for future compound optimization.

■ ASSOCIATED CONTENT

SI Supporting Information

The Supporting Information is available free of charge at <https://pubs.acs.org/doi/10.1021/acsmchemlett.2c00249>.

Details of the computational protocols, synthetic procedures, analytical data, and biological assays (PDF)

■ AUTHOR INFORMATION

Corresponding Authors

Elena Petricci – Dipartimento di Biotecnologie Chimica e Farmacia, Università di Siena, I-53100 Siena, Italy;

Phone: +39 0577 232417; Email: elena.petricci@unisi.it

Barbara Stecca – Istituto per lo Studio, la Prevenzione e la Rete Oncologica (ISPRO), I-50139 Firenze, Italy;

orcid.org/0000-0003-1197-1622; Phone: +39 055 7944567; Email: b.stecca@ispro.toscana.it

Fabrizio Manetti – Dipartimento di Biotecnologie Chimica e Farmacia, Università di Siena, I-53100 Siena, Italy;

orcid.org/0000-0002-9598-2339; Phone: +39 0577 234330; Email: fabrizio.manetti@unisi.it

Authors

Luisa Maresca – Istituto per lo Studio, la Prevenzione e la Rete Oncologica (ISPRO), I-50139 Firenze, Italy

Enrica Crivaro – Istituto per lo Studio, la Prevenzione e la Rete Oncologica (ISPRO), I-50139 Firenze, Italy;

orcid.org/0000-0002-6098-3315

Sara Pepe – Istituto per lo Studio, la Prevenzione e la Rete Oncologica (ISPRO), I-50139 Firenze, Italy

Elena Cini – Dipartimento di Biotecnologie Chimica e Farmacia, Università di Siena, I-53100 Siena, Italy;

orcid.org/0000-0003-4420-8930

Snigdha Singh – Dipartimento di Biotecnologie Chimica e Farmacia, Università di Siena, I-53100 Siena, Italy

Paolo Governa – Dipartimento di Biotecnologie Chimica e Farmacia, Università di Siena, I-53100 Siena, Italy;

orcid.org/0000-0002-5976-780X

Samuele Maramai – Dipartimento di Biotecnologie Chimica e Farmacia, Università di Siena, I-53100 Siena, Italy;

orcid.org/0000-0001-7499-6961

Giuseppe Giannini – R&D, Alfasigma SpA, I-00071 Roma, Italy; orcid.org/0000-0002-7127-985X

Complete contact information is available at:

<https://pubs.acs.org/doi/10.1021/acsmchemlett.2c00249>

Author Contributions

The manuscript was written through contributions of all authors. All authors have given approval to the final version of the manuscript.

Funding

This work was supported in part by the research grant from the AIRC foundation (grant IG 2017 n. 20758), by the project “Development and application of QM/MM technologies for the design of light responsive proteins or protein-mimics based on rhodopsin architecture” within the program “Dipartimenti di Eccellenza -2018–2022 financed by MIUR (Roma, Italy)

and by Bando Ricerca Salute 2018 financed by Tuscany Region (project GLI SELTHER). We are grateful for funding obtained from the Institute for Cancer Research, Prevention and Clinical Network (ISPRO). L. Maresca is supported by a postdoctoral fellowship from the Italian Association for Cancer Research (AIRC, project n. 22644). Additional financial support was provided by Leadiant Biosciences S.A. (Mendrisio, CH) (formerly Sigma-Tau Research Switzerland, S.A.). The MIUR research project 2015LZE994 (Insights into the functions of DNA damage processing and repair factors to design novel selective anticancer drugs) is also acknowledged.

Notes

The authors declare the following competing financial interest(s): G. Giannini participated in the project as Project Leader, thanks to the agreement signed between Leadiant Bioscience and Sigma-Tau IFR SpA (now Alfasigma SpA). Part of the results described herein has been the subject of a patent application: "GLI inhibitors and uses thereof" Application No EP 17166194.5 April 12, 2017. EP3388419A1. Giannini, G.; Taddei, M.; Manetti, F.; Petricci, E.; Stecca, B.

ACKNOWLEDGMENTS

The authors would like to thank Dr. G. Battistuzzi (R&D Alfasigma S.p.A., formerly Sigma-Tau IFR S.p.A) for assistance with a few aspects of this project, Dr. A. Nosedà (Leadiant Biosciences SA) for facilitating this study, as well as Dr. E. Monciatti and F. Migliorini for some NMR analyses. Glabrescione B was a gift from B. Botta and L. Di Marcotullio, University of Rome La Sapienza.

ABBREVIATIONS

Hh, Hedgehog; PTCH1, Patched; SMO, Smoothed; TF, transcription factor; GlaB, glabrescione B; CDI, *N,N'*-carbon-diimidazole

REFERENCES

- (1) Pietrobono, S.; Gagliardi, S.; Stecca, B. Non-canonical Hedgehog signaling pathway in cancer: activation of GLI transcription factors beyond Smoothed. *Front. Genet.* **2019**, *10*, 556.
- (2) Danhof, R.; Lewis, K.; Brown, M. Small molecule inhibitors of the Hedgehog pathway in the treatment of basal cell carcinoma of the skin. *Am. J. Clin. Dermatol.* **2018**, *19*, 195–207.
- (3) Nguyen, N. M.; Cho, J. Hedgehog pathway inhibitors as targeted cancer therapy and strategies to overcome drug resistance. *Int. J. Mol. Sci.* **2022**, *23*, 1733.
- (4) Avery, J. T.; Zhang, R.; Boohaker, R. J. GLI1: a therapeutic target for cancer. *Front. Oncol.* **2021**, *11*, 673154.
- (5) Peer, E.; Tesanovic, S.; Aberger, F. Next-generation Hedgehog/GLI pathway inhibitors for cancer therapy. *Cancers* **2019**, *11*, 538.
- (6) Zhang, R.; Ma, J.; Avery, J. T.; Sambandam, V.; Nguyen, T. H.; Xu, B.; Suto, M. J.; Boohaker, R. J. GLI1 inhibitor SRI-38832 attenuates chemotherapeutic resistance by downregulating NBS1 transcription in BRAF^{V600E} colorectal cancer. *Front. Oncol.* **2020**, *10*, 241.
- (7) Lospinoso Severini, L.; Ghirga, F.; Bufalieri, F.; Quaglio, D.; Infante, P.; Di Marcotullio, L. The SHH/GLI signaling pathway: a therapeutic target for medulloblastoma. *Expert Opin. Ther. Targets* **2020**, *24*, 1159–1181.
- (8) Bariwal, J.; Kumar, V.; Dong, Y.; Mahato, R. I. Design of Hedgehog pathway inhibitors for cancer treatment. *Med. Res. Rev.* **2019**, *39*, 1137–1204.
- (9) Hyman, J. M.; Firestone, A. J.; Heine, V. M.; Zhao, Y.; Ocasio, C. A.; Han, K.; Sun, M.; Rack, P. G.; Sinha, S.; Wu, J. J.; Solow-Cordero, D. E.; Jiang, J.; Rowitch, D. H.; Chen, J. K. Small-molecule inhibitors

reveal multiple strategies for Hedgehog pathway blockade. *Proc. Natl. Acad. Sci. U.S.A.* **2009**, *106*, 14132–14137.

(10) Mastrangelo, E.; Milani, M. Role and inhibition on GLI1 protein in cancer. *Lung Cancer Targets Ther.* **2018**, *9*, 35–43.

(11) Lauth, M.; Bergström, A.; Shimokawa, T.; Toftgård, R. Inhibition of GLI-mediated transcription and tumor cell growth by small-molecule antagonists. *Proc. Natl. Acad. Sci. U.S.A.* **2007**, *104*, 8455–8460.

(12) Agyeman, A.; Jha, B. K.; Mazumdar, T.; Houghton, J. A. Mode and specificity of binding of the small molecule GANT61 to GLI determines inhibition of GLI-DNA binding. *Oncotarget* **2014**, *5*, 4492–4503.

(13) Kim, J.; Lee, J. J.; Kim, J.; Gardner, D.; Beachy, P. A. Arsenic antagonizes the Hedgehog pathway by preventing ciliary accumulation and reducing stability of the Gli2 transcriptional effector. *Proc. Natl. Acad. Sci. U.S.A.* **2010**, *107*, 13432–13437.

(14) Cai, X.; Yu, K.; Zhang, L.; Li, Y.; Li, Q.; Yang, Z.; Shen, T.; Duan, L.; Xiong, W.; Wang, W. Synergistic inhibition of colon carcinoma cell growth by Hedgehog-Gli1 inhibitor arsenic trioxide and phosphoinositide 3-kinase inhibitor LY294002. *Oncotargets Ther.* **2015**, *8*, 877–883.

(15) Comba, A.; Almada, L. L.; Tolosa, E. J.; Iguchi, E.; Marks, D. L.; Vara Messler, M.; Silva, R.; Fernandez-Barrena, M. G.; Enriquez-Hesles, E.; Vrabel, A. L.; Botta, B.; Di Marcotullio, L.; Ellenrieder, V.; Eynard, A. R.; Pasqualini, M. E.; Fernandez-Zapico, M. F. Nuclear factor of activated T cells-dependent down-regulation of the transcription factor glioma-associated protein 1 (GLI1) underlies the growth inhibitory properties of arachidonic acid. *J. Biol. Chem.* **2016**, *291*, 1933–1947.

(16) Chai, J. Y.; Sugumar, V.; Alshawsh, M. A.; Wong, W. F.; Arya, A.; Chong, P. P.; Looi, C. Y. The role of Smoothed-dependent and -independent Hedgehog signaling pathway in tumorigenesis. *Bio-medicines* **2021**, *9*, 1188.

(17) Infante, P.; Mori, M.; Alfonsi, R.; Ghirga, F.; Aiello, F.; Toscano, S.; Ingallina, C.; Siler, M.; Cucchi, D.; Po, A.; Miele, E.; D'Amico, D.; Canettieri, G.; De Smaele, E.; Ferretti, E.; Screpanti, I.; Uccello Barretta, G.; Botta, M.; Botta, B.; Gulino, A.; Di Marcotullio, L. GLI1/DNA interaction is a druggable target for Hedgehog-dependent tumors. *EMBO J.* **2015**, *34*, 200–217.

(18) Manetti, F.; Stecca, B.; Santini, R.; Maresca, L.; Giannini, G.; Taddei, M.; Petricci, E. Pharmacophore-based virtual screening for identification of negative modulators of GLI1 as potential anticancer agents. *ACS Med. Chem. Lett.* **2020**, *11*, 832–838.

(19) Dash, R. C.; Wen, J.; Zaino, A. M.; Morel, S. R.; Chau, L. Q.; Wechsler-Reya, R. J.; Hadden, K. M. Structure-based virtual screening identifies an 8-hydroxyquinoline as a small molecule GLI1 inhibitor. *Mol. Ther. Oncolytics* **2021**, *20*, 265–276.

(20) Manetti, F.; Faure, H.; Roudaut, H.; Gorojankina, T.; Traiffort, E.; Schoenfelder, A.; Mann, A.; Solinas, A.; Taddei, M.; Ruat, M. Virtual screening-based discovery and mechanistic characterization of the acylthiourea MRT-10 family as Smoothed antagonists. *Mol. Pharmacol.* **2010**, *78*, 658–665.

(21) Badolato, M.; Carullo, G.; Perri, M.; Cione, E.; Manetti, F.; Di Gioia, M. L.; Brizzi, A.; Caroleo, M. C.; Aiello, F. Quercetin/oleic acid-based G-protein-coupled receptor 40 ligands as new insulin secretion modulators. *Fut. Med. Chem.* **2017**, *9*, 1873–1885.

(22) Cione, E.; Caroleo, M. C.; Kagechika, H.; Manetti, F. Pharmacophore-guided repurposing of fibrates and retinoids as GPR40 allosteric ligands with activity on insulin release. *J. Enz. Inhib. Med. Chem.* **2021**, *36*, 377–383.

(23) Pavletich, N. P.; Pabo, C. O. Crystal structure of a five-finger GLI-DNA complex: new perspectives on zinc fingers. *Science* **1993**, *261*, 1701–1707.